



Han, X., Tomaszewski, E. J., Sorwat, J., Pan, Y., Kappler, A., & Byrne, J. M. (2020). Effect of Microbial Biomass and Humic Acids on Abiotic and Biotic Magnetite Formation. *Environmental Science and Technology*, 54, 4121-4130. [7].
<https://doi.org/10.1021/acs.est.9b07095>

Peer reviewed version

Link to published version (if available):
[10.1021/acs.est.9b07095](https://doi.org/10.1021/acs.est.9b07095)

[Link to publication record in Explore Bristol Research](#)
PDF-document

This is the author accepted manuscript (AAM). The final published version (version of record) is available online via American Chemical Society at <https://pubs.acs.org/doi/10.1021/acs.est.9b07095> . Please refer to any applicable terms of use of the publisher.

University of Bristol - Explore Bristol Research

General rights

This document is made available in accordance with publisher policies. Please cite only the published version using the reference above. Full terms of use are available:
<http://www.bristol.ac.uk/red/research-policy/pure/user-guides/ebr-terms/>

Effect of Microbial Biomass and Humic Acids on Abiotic and Biotic Magnetite Formation

Xiaohua Han^{1,2,3,4,5}, Elizabeth J. Tomaszewski², Julian Sorwat², Yongxin Pan^{1,3,4,5}, Andreas Kappler², James M. Byrne^{2*}

¹ *Biogeomagnetism Group, Key Laboratory of Earth and Planetary Physics, Institute of Geology and Geophysics, Chinese Academy of Sciences, Beijing 100029, China*

² *Geomicrobiology, Center for Applied Geosciences, University of Tuebingen, 72074 Tuebingen, Germany*

³ *France-China International Laboratory of Evolution and Development of Magnetotactic Multicellular Organisms, Chinese Academy of Sciences, Beijing 100029, China*

⁴ *Institutions of Earth Science, Chinese Academy of Sciences, China*

⁵ *College of Earth and Planetary Sciences, University of Chinese Academy of Sciences, Beijing 100049, China*

*corresponding author: james.byrne@uni-tuebingen.de

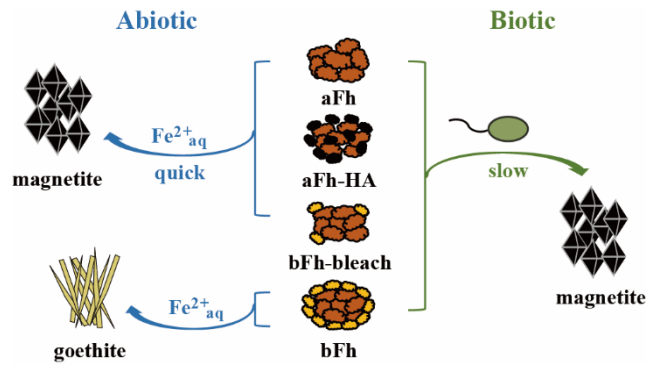
For submission to: Environmental Science & Technology

ABSTRACT

Magnetite (Fe_3O_4) is an environmentally ubiquitous mixed-valent iron (Fe) mineral which can form via biotic or abiotic transformation of Fe(III) (oxyhydr)oxides such as ferrihydrite (Fh). It is currently unclear whether environmentally relevant biogenic Fh from Fe(II)-oxidizing bacteria, containing cell-derived organic matter, can transform to magnetite. We compared abiotic and biotic transformation: 1) abiogenic Fh (aFh); 2) abiogenic Fh coprecipitated with humic acids (aFh-HA); 3) biogenic Fh produced by phototrophic Fe(II)-oxidizer *Rhodobacter ferrooxidans* SW2 (bFh); 4) biogenic Fh treated with bleach to remove biogenic organic matter (bFh-bleach). Abiotic or biotic transformation of Fh was promoted by $\text{Fe}^{2+}_{\text{aq}}$ or Fe(III)-reducing bacteria. $\text{Fe}^{2+}_{\text{aq}}$ -catalyzed abiotic reaction with aFh and bFh-bleach led to complete transformation to magnetite. In contrast, aFh-HA only partially (68%) transformed to magnetite, and bFh (17%) transformed to goethite. We hypothesize that microbial biomass stabilized bFh against reaction with $\text{Fe}^{2+}_{\text{aq}}$. All four Fh substrates were transformed into magnetite during biotic reduction, suggesting that Fh remains bioavailable even when associated with microbial biomass. Additionally, there were poorly ordered magnetic components detected in the biogenic end-products for aFh and aFh-HA. Nevertheless, abiotic transformation was much faster than biotic transformation, implying that initial $\text{Fe}^{2+}_{\text{aq}}$ concentration, passivation of Fh and/or sequestration of Fe(II) by bacterial cells and associated biomass play major roles in the rate of magnetite formation from Fh. These results improve our understanding of factors influencing secondary mineralization of Fh in the environment.

Key words: Biogenic ferrihydrite, biogeochemical cycling, secondary mineral transformation, magnetic susceptibility

Graphical Abstract



INTRODUCTION

Magnetite (Fe_3O_4), a mixed-valent magnetic mineral containing both Fe(II) and Fe(III) in a ratio of 1:2, is widespread in environments such as soils and sediments.¹ Magnetite is bioavailable, serving as an electron sink or electron source for Fe(II)-oxidizing and Fe(III)-reducing bacteria respectively, contributing to biogeochemical cycling of Fe in terrestrial and aquatic environments.^{2, 3} Additionally, the unique properties of magnetite allow for its use in many diverse applications including medical treatments, carbon sequestration, and groundwater remediation.⁴⁻⁶ Thus, understanding the formation mechanisms of magnetite in the environment is beneficial for understanding biogeochemical cycling of Fe, and also for developing new bioinspired materials for industrial applications.

In natural environments, magnetite can be formed via abiotic or biotic mechanisms including biotic transformation of Fe(III) (oxyhydr)oxide minerals such as ferrihydrite (Fh).^{2, 7, 8} $\text{Fe}^{2+}_{\text{aq}}$ and dissimilatory Fe(III)-reducing bacteria can promote the transformation of Fh to magnetite or other crystalline ferric minerals, such as lepidocrocite ($\gamma\text{-FeOOH}$), goethite ($\alpha\text{-FeOOH}$), or hematite ($\alpha\text{-Fe}_2\text{O}_3$), depending on geochemical conditions (e.g. $\text{Fe}^{2+}_{\text{aq}}$ concentration, pH or the presence of ligands).⁹⁻¹³

In soil environments, Fh is often associated with natural organic matter (NOM), which is frequently approximated in laboratory studies by humic acids (HA), a chemically isolated subfraction of NOM.^{8, 14, 15} Fh may be reduced by NOM either abiotically (via reduced functional groups present in NOM such as hydroquinones) or, more often, microbially by microorganisms using this organic matter as a carbon substrate.^{16, 17} Previous experiments studying abiotic reduction of Fh containing adsorbed organic matter or coprecipitated with organic matter showed decreasing initial Fe(III) reduction rates and degrees of reduction with increasing amounts of mineral-bound organic matter.¹⁸⁻²¹ For biotic reduction of OM- Fh substrates, the effects of OM on Fh transformation to secondary phases depended on the extent OM acted as an electron shuttle for microbes, and the extent of surface site blocking and/or

aggregation.²²⁻²⁴ In the environment, OM may also be associated with Fe minerals as a byproduct of Fe(II)-oxidizing bacteria, for example photoferrotrophs which can harvest light energy and oxidize Fe(II) to Fe(III) (oxyhydr)oxides. This OM is usually associated with biogenic Fe(III) (oxyhydr)oxides (i.e. ferrihydrite) in oxygen-limited anoxic sediments, such as creeks, rhizosphere and wetland systems.²⁵⁻²⁸ The incorporation and/or surface aggregation of biomass can substantially impact mineral properties and transformation pathways of biogenic Fe(III) (oxyhydr)oxides.²⁰ However, little is known about the effects of microbial biomass on the reductive transformation pathways of biogenic Fe(III) (oxyhydr)oxides.

The main objective of this study was to assess the factors governing the rates and extent of abiotic and biotic reductive transformation of OM-ferrihydrite to magnetite in order to understand how such OM-mineral associations might influence biogeochemical Fe cycling in the environment. Here, we studied the abiotic and biotic transformation of abiogenic and biogenic Fh, with and without OM by $\text{Fe}^{2+}_{\text{aq}}$ or Fe(III)-reducing bacteria *Shewanella oneidensis* MR-1, respectively. We monitored Fh transformation over time by following Fe redox speciation with the spectrophotometric ferrozine assay, magnetic susceptibility, and analysed the transformation products by Mössbauer spectroscopy.

MATERIALS AND METHODS

Preparation of Fh substrates. Abiogenic ferrihydrite (aFh) was precipitated by reaction of $\text{Fe}(\text{NO}_3)_3 \cdot 9\text{H}_2\text{O}$ (40 g) with KOH (1 M) until pH 7.5.²⁹ The material was centrifuged (7500 rpm; 10 min) and washed in ultrapure H_2O (Milli-Q) to remove nitrate ions, with washing repeated three times. Abiogenic ferrihydrite coprecipitated with humic acids (aFh-HA) was synthesized following a similar approach as for aFh, except 3.26 g humic acids (Sigma-Aldrich, H16752) was added into $\text{Fe}(\text{NO}_3)_3 \cdot 9\text{H}_2\text{O}$ (40 g) before addition of KOH (1 M). The mass of HA was chosen to ensure that the C/Fe ratio of aFh-HA matched that of bFh (see section: Mineral characterization), which allows aFh-HA as more of an analogue to biogenic Fh using

abiogenic synthesis procedures. Biogenic ferrihydrite (bFh) was produced from Fe(II) oxidation by the phototrophic Fe(II)-oxidizer *Rhodobacter ferrooxidans* SW2.³⁰ The mineral precipitate was centrifuged and washed with ultrapure H₂O to remove ions and loosely associated bacteria from the medium, with the washing step repeated three times. Organic matter free biogenic ferrihydrite (bFh-bleach) was obtained by exposing bFh to 6% NaOCl to remove biogenic organic matter. This treatment was repeated up to 6 times, rolling at 40 rpm/min for 6 hours during each treatment and decanting the supernatant solution after centrifugation.³¹ The treated samples were washed in ultrapure H₂O to remove NaOCl. The Fe total concentration of all four starting materials was determined by chemical dissolution (1 M HCl) followed by the spectrophotometric ferrozine assay.³²

Strains and medium. Information about microbial strains and cultivation is provided in the SI.

Incubation experiments. Abiotic experiments were performed in 50 ml serum bottles with 10 mM anoxic HEPES buffer, 3 mM Fh and 7 mM FeCl₂. For biotic experiments, a cell suspension of *S. oneidensis* MR-1 with cell concentration 5×10⁸ cells/mL was added to 10 mmol/L Fh with 9 mM lactate as electron donor in anoxic HEPES buffer (10 mM; pH 7.2). Triplicate experiments were used for Fe concentration quantification, and another set of triplicates were used for magnetic susceptibility (MS) measurements for each batch reactor. Separate bottles were required for MS because removal of solid material for Fe quantification interferes with MS analysis. Control bottles containing no Fe²⁺_{aq} or inoculum were included to confirm the absence of spontaneous transformation of Fh. All experiments were incubated at 28°C in darkness. Figure S1 gives further details of all batch reactors with the four Fh substrates under abiotic and biotic reductive conditions.

Mineral characterization. The specific surface area (SSA) of the four Fh substrates was determined by the Brunauer-Emmett-Teller (BET) method (Gemini VII Surface Area and Porosity Analyzer, Micromeritics, Germany). Fh substrates were analyzed by N₂ adsorption at 77 K after the samples were dried at 60°C in an oven. For zeta potential (ZP) measurement, the

four Fh substrates were diluted with 10 mM HEPES buffer, which was adjusted to pH 7.2 in order to have the same pH as in the initial medium. All measurements were conducted using a Zetasizer Nano ZSP with Zetasizer Nano Series disposable folded capillary cells (DTS1070; Malvern, Herrenberg, Germany). Total organic carbon (TOC) was quantified using a TOC analyzer (Model 2100S, Analytik Jena, Germany) after the samples were dried at 60°C in an oven. For Mössbauer analysis, samples of four Fh substrates and final mineral products were filtered on 0.45 µm filter papers and embedded in Kapton tape in a glovebox (100% N₂). These samples were stored in anoxic air-tight bottles at -20°C until analysis. The samples were measured at 140 K using a ⁵⁷Fe Mössbauer spectrometer (WissEL) with a ⁵⁷Co/Rh source. Spectra were fitted using the Voigt based fitting (VBF) routine in the Recoil software (University of Ottawa).³³

Fe concentration quantification and Magnetic susceptibility. Information about Fe concentration quantification and in-situ volume-dependent magnetic susceptibility (MS) measurements is provided in the SI.

Calculation of delay between Fh reduction and magnetite formation (Δt). In order to determine the differences between the increase in Fe(II)/Fe(III) ratio and increase in MS for the four Fh substrates in abiotic and biotic transformation experiments, the Fe(II)/Fe(III) and MS triplicate average values for individual batch reactors over time were fitted with the Hill equation (see Supporting Information), with the first order derivative calculated using Origin Pro 2017.

RESULTS

Ferrihydrite substrate properties. Mössbauer spectroscopy of all four Fh substrates at 140 K (Figure S2) were characterized by doublets with hyperfine parameters that were indicative of ferrihydrite, with some potential interparticle interactions such as formation of larger aggregates due to HA and microbial biomass in samples aFh-HA and bFh.¹⁹ C content, specific surface area (SSA), and zeta potential for ferrihydrite substrates are given in Table S1. TOC analyses revealed the C/Fe molar ratio of bFh and aFh-HA to be similar (0.39 and 0.42) while that of aFh and bFh-bleach were close to zero. The similarity of C/Fe and mineralogy of aFh and bFh-bleach suggests that the bleach (NaOCl) was successful at removing ~97% biomass in bFh without affecting the mineralogical phase, although this cannot be fully confirmed without a more thorough analysis using high resolution methods (e.g. high resolution transmission electron microscopy) which fall beyond the scope of this study. Due to the blockage of mineral surface sites by HA, as well as the formation of larger aggregates, aFh-HA had much lower SSA, 13 m²/g, compared to aFh (306 m²/g). Similarly, the surface charge for aFh-HA was very negative at -21.7 mV, while that of aFh was positive with +12.7 mV. The surface charge for bFh was also negative with -27.0 mV due to the presence of biomass. However, although the C/Fe molar ratios of bFh and aFh-HA were similar, the SSA of bFh (228 m²/g) was not as low as that of aFh-HA, which implies that the extent of mineral surface site blockage by biomass and/or formation of aggregates was lower for bFh than for aFh-HA. Given that NaOCl removed ~97% biomass in bFh, the bFh-bleach had slightly higher SSA (255 m²/g) than bFh and a more positive surface charge with +2.60 mV.

Fh reduction and transformation over time. Variations of Fe²⁺_{aq} for both abiotic and biotic transformation of the four Fh substrates as well as the variations of solid-phase Fe(II)/Fe(III) ratio of abiotic and biotic transformation are shown in Figure 1. The solid-phase Fe(II)/Fe(III) ratio was the ratio between total Fe(II) (including structural Fe(II) and adsorbed Fe(II)) and

total Fe(III) (including structural Fe(III) and adsorbed Fe(III)) which were determined by the spectrophotometric ferrozine assay. No $\text{Fe}^{3+}_{\text{aq}}$ was detected in any experiment. Detailed data are included in the SI.

In the abiotic transformation experiment $\text{Fe}^{2+}_{\text{aq}}$ decreased over time, likely due to adsorption and reaction with Fh. The Fe(II)/Fe(III) ratios at the first measured time point (0.5 h) for all four Fh substrates were ~0.2 (i.e. not zero), suggesting adsorption of $\text{Fe}^{2+}_{\text{aq}}$. The Fe(II)/Fe(III) ratio of aFh rapidly increased to 0.43 over 6 hours, and more slowly to 0.46 over 14 days. Compared with aFh, the Fe(II)/Fe(III) ratio of aFh-HA and bFh-bleach increased more slowly to 0.42 and 0.47 in 14 days respectively. Conversely, the Fe(II)/Fe(III) ratio for bFh only increased to 0.08 in 56 days, even though some $\text{Fe}^{2+}_{\text{aq}}$ was adsorbed to the mineral surface at the beginning of experiment.

In the biotic transformation experiments, the $\text{Fe}^{2+}_{\text{aq}}$ concentration in batch reactors containing aFh-HA, bFh and bFh-bleach were higher (1.3-1.47 mM) than in that with aFh (1.03 mM) after 36 days. This is likely because $\text{Fe}^{2+}_{\text{aq}}$ produced in these batch reactors could not react with Fh either due to surface site blockage by HA or biomass, or potentially due to changes to the surface reactivity of bFh-bleach during bleach treatment which were not detectable via Mössbauer spectroscopy. However, after 153 days, there were decreases of $\text{Fe}^{2+}_{\text{aq}}$ indicating that the Fe(II) produced by *S. oneidensis* adsorbed to and reacted with the Fh. The Fe(II)/Fe(III) ratio of aFh increased rapidly to 0.43 over 52 hours, and kept increasing more slowly to 0.52 over 36 days. Compared with aFh, the Fe(II)/Fe(III) ratio of aFh-HA and bFh-bleach increased more slowly reaching 0.52 in 7 days and 0.45 in 14 days, respectively, and kept increasing to 0.81 and 0.96 over 153 days. The Fe(II)/Fe(III) ratio of bFh continuously increased to 2.28 in 153 days. Only Fe(II)/Fe(III) of aFh was close to the stoichiometric magnetite ratio of 0.5, while the other three Fh substrates showed much higher values (0.96 for aFh-HA, 2.28 for bFh, 0.81 for bFh-bleach), suggesting that magnetite might not have been the only transformation product.

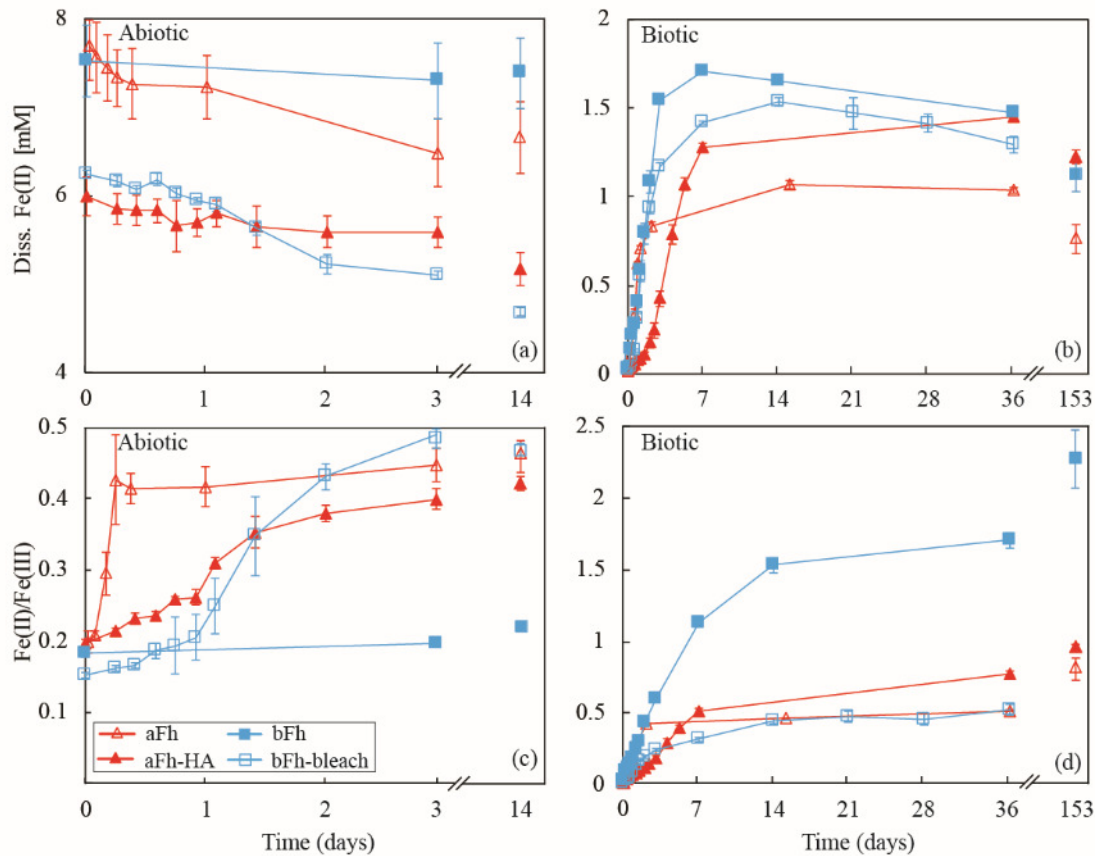


Figure 1. Ferrihydrite transformation promoted by $\text{Fe}^{2+}_{\text{aq}}$ or Fe(III)-reducing bacteria *S. oneidensis* MR-1, respectively. (a) and (b) are $\text{Fe}^{2+}_{\text{aq}}$ concentration in abiotic and biotic transformations of ferrihydrite; (c) and (d) are solid phase Fe(II)/Fe(III) ratios over time in abiotic and biotic transformation of ferrihydrite. Error bars indicate range of triplicate culture bottles. Bars not visible are smaller than the symbols. Please note the different time scales for abiotic and biotic batch reactors.

Magnetic susceptibility (MS) results for abiotic and biotic transformation are shown in Figure 2. Changes to magnetic susceptibility in the experimental batch reactors matched expected changes based on $\text{Fe}^{2+}_{\text{aq}}$ concentrations and Fe(II)/Fe(III) ratios described above. A previous study on in-situ magnetic susceptibility measurements showed MS measurements to be suitable for following microbial Fe(III) mineral transformation, in particular magnetite formation and transformation.³⁴ Given the composition of the media (only lactate and HEPES

buffer were present), we expect that only the formation of ferrimagnetic magnetite will contribute to high increases in MS. Thermodynamically stable minerals goethite, hematite and remaining paramagnetic minerals such as starting ferrihydrite have a much smaller, positive MS.

In abiotic experiments, the MS of aFh increased rapidly to 935×10^{-6} SI in only 3 hours. The following decrease to 559×10^{-6} SI (43% decrease compared to the maximum MS) by day 22 likely indicates an increase of magnetite grain size. If part of the magnetite particles grow above the critical volume of the superparamagnetic to single domain transition, the overall MS value of the sample could decrease because of the lower MS of single domain particles compared to the smaller superparamagnetic grains.³⁵ Similarly, the MS of bFh-bleach increased rapidly to 896×10^{-6} SI in 1 day followed by a decrease to 755×10^{-6} SI by day 22 (16% decrease compared to maximum MS). For aFh-HA, MS increased to 834×10^{-6} SI in 2 days and continued to slowly increase to 963×10^{-6} SI over 22 days. However, there was no MS change of bFh during 64 days, which is consistent with the Fe(II)/Fe(III) ratio of bFh, implying that microbial biomass present in bFh blocked the reaction between bFh and $\text{Fe}^{2+}_{\text{aq}}$.

In biotic Fh reduction experiments, the MS of aFh increased rapidly to 3345×10^{-6} SI in 2 days and decreased to 2871×10^{-6} SI (14% decrease compared to the maximum MS) after 47 days, similar to aFh in the abiotic experiment. Increasing trends of MS for aFh-HA, bFh and bFh-bleach were similar in which MS increased quickly in the first 133 days and kept slowly increasing until 278 days. The final MS value of bFh (1070×10^{-6} SI) in the biotic transformation experiment was similar with that of the other three Fh substrates in abiotic transformation, which owing to the fact that the final Fe(III) concentrations in the solid phase were also similar (2.8 ± 0.2 mM), suggests a similar amount of magnetite was likely produced. The final MS values of aFh, aFh-HA and bFh-bleach were higher (2871×10^{-6} SI, 4222×10^{-6} SI and 2441×10^{-6} SI).

⁶SI respectively) than that of bFh in biotic transformation, and had correspondingly higher final solid Fe(III) (3.4-4.6 mM).

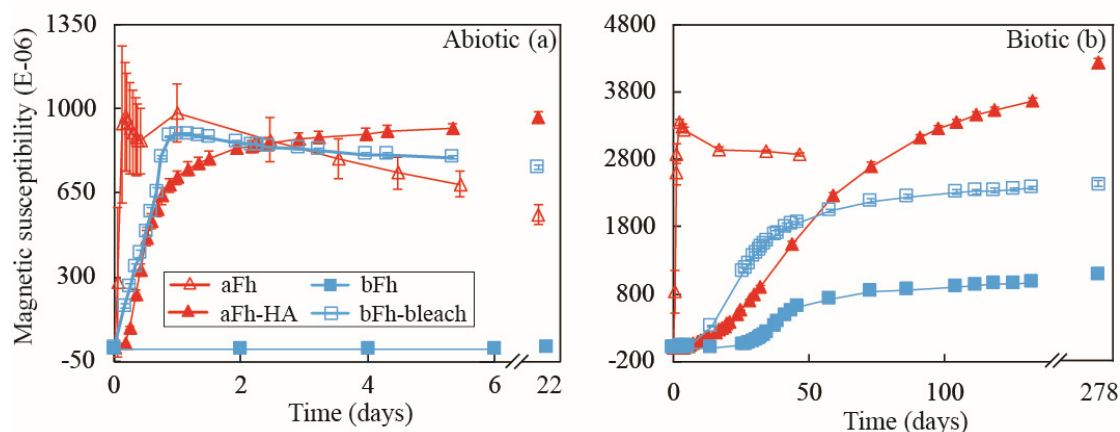


Figure 2. Magnetic susceptibility (MS) over time in abiotic (a) and biotic (b) transformation of ferrihydrite. Error bars indicate range of triplicate culture bottles. Bars not visible are smaller than the symbols. Please note the different time scales for the abiotic and biotic batch reactors.

Identity of Fh transformation products. 140 K Mössbauer spectra of transformation products are shown in Figure 3, with corresponding fit parameters presented in Table S2. Our data showed that the solid-phase products formed during Fe(II)-catalyzed abiotic transformation and during dissimilatory iron reduction of ferrihydrite by *S. oneidensis* MR-1 were goethite and magnetite, sometimes associated with a strong Fe(II) doublet in Mössbauer spectra, the identity of which cannot be accurately determined but likely corresponds to Fe(II) which adsorbed to the mineral surface. Some spectra also required the inclusion of a poorly ordered magnetic phase. This phase potentially represents either superparamagnetic magnetite, or goethite which have not undergone full magnetic ordering at 140 K. The Fe(II)-catalyzed abiotic transformation of aFh and bFh-bleach led to complete transformation to magnetite, which is consistent with the Fe concentration results for aFh and bFh-bleach in which the solid-phase

Fe(II)/Fe(III) ratios for both Fh were close to 0.5 which is the stoichiometric Fe(II)/Fe(III) ratio of magnetite. In contrast, aFh-HA only underwent partial transformation to magnetite (68.2%), with paramagnetic Fe(III) (28.5%) and Fe(II) (3.3%) remaining in the solids after 22-days cultivation. The bFh underwent further transformation into more thermodynamically stable goethite (16.7%); however, no magnetite was produced within 64 days.

Conversely, all four Fh substrates were transformed into magnetite during biotic Fe(III) reduction, although not to completion. Evidence of remaining Fh suggests that even though the HA and biomass associated Fh is bioavailable, the organic matter still partially prevents transformation of Fh to magnetite. The maximum transformation extent of Fh in the biotic experiment is 68.5% for the bFh-bleach phase. Although aFh had no organic matter, there was a lower relative abundance of magnetite (~62.3%) produced compared to bFh-bleach with paramagnetic Fe accounting for the remaining spectral area. For aFh-HA and bFh, nearly half of the Fe was present as magnetite, at 49.9% and 56.1%, respectively.

The Fe(II)/Fe(III) ratio of each of the magnetite formation products was determined based on Mössbauer spectroscopy and is shown in Table S3.³⁶ The ratios varied between samples, with aFh-HA (biotic) having lowest value of 0.33, suggesting that stoichiometric magnetite was not formed. In contrast, bFh-bleach (biotic) had the highest Fe(II)/Fe(III) ratio of 0.54 which suggests a relatively reduced magnetite. In the only two samples which converted completely to magnetite without any additional transformation products, the ratios were calculated to be 0.45 and 0.40 for aFh and bFh-bleach (abiotic), respectively. This suggests that magnetite formed from the bleach-washed biogenic ferrihydrite is partially oxidized in comparison to the pure ferrihydrite. However, no clear pattern emerged which suggests that abiotic or biotic reactions favor either more reduced or more oxidized magnetite.

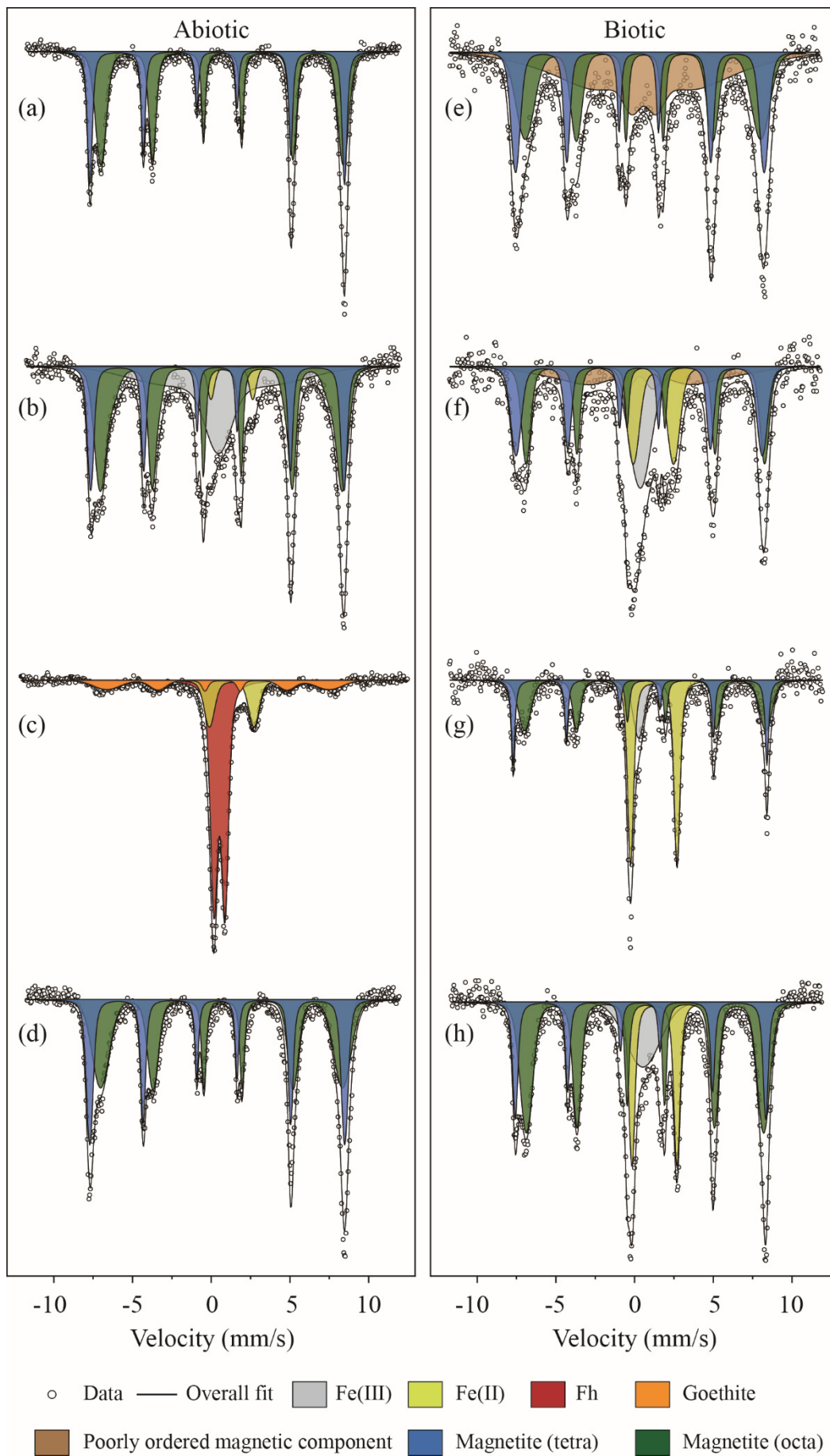


Figure 3. Mössbauer spectra of ferrihydrite transformation induced by $\text{Fe}^{2+}_{\text{aq}}$ abiotically ((a)-(d)) and *S. oneidensis* MR-1 biotically ((e)-(h)). (a)(e) are aFh transformation products; (b)(f) are aFh-HA transformation products; (c)(g) are bFh transformation products; (d)(h) are bFh-bleach transformation products. Open circles: measured data, solid line: fitted spectrum, filled areas: modelled relative amounts of identified minerals.

DISCUSSION

Role of initial $\text{Fe}^{2+}_{\text{aq}}$ concentration and Fe(II)/Fh ratio in Fh transformation. Abiotic transformation was faster compared to biotic transformation, implying that the initial $\text{Fe}^{2+}_{\text{aq}}$ plays a dominant role in the rate of magnetite formation from Fh. Previous studies on Fe(II)-induced abiotic transformation of ferrihydrite showed that magnetite accumulation is only observed at $\text{Fe}^{2+}_{\text{aq}}$ concentration exceeding 0.3 mM (equivalent to 0.5 mmol Fe[II]/g ferrihydrite); otherwise only lepidocrocite and/or goethite formed after 140 hours.^{7, 12} In our abiotic experiments, we cannot rule out the possibility that lepidocrocite and/or goethite formed as intermediate products. However, given the Fe(II) concentration (Fe(II) to Fh ratio was 2.3, equivalent to 28 mmol Fe[II]/g ferrihydrite) and long duration of experiments (more than 510 hours) such phases might have undergone transformation to magnetite and are thus not visible in the Mössbauer spectra. This initial $\text{Fe}^{2+}_{\text{aq}}$ concentration was based on our abiotic preliminary experiments in which $\text{Fe}^{2+}_{\text{aq}}$ was reacted with aFh at different Fe(II)/Fe(III) ratios (ranging from 0.5 to 10). In these preliminary experiments, MS results showed that no magnetite formed when the Fe(II)/Fe(III) ratio was 0.5, and neither when the Fe(II)/Fe(III) ratio was 10 (Figure S3). Although the Fe(II)/Fe(III) ratio of 0.5 (equivalent to 6 mmol Fe[II]/g ferrihydrite) is higher than that required for magnetite nucleation,⁷ the absence of any increase of MS implied that no magnetite was produced. Therefore, we speculate that there were Fe(III) (oxyhydr)oxides with lower MS, such as lepidocrocite or goethite, transformed from Fh when the initial Fe(II)/Fe(III) is too low (lower than 0.5) to initiate nucleation of magnetite. When the initial

Fe(II)/Fe(III) is high (higher than 10), the rate of reduction was so fast, that all Fh substrate was used by the bacteria, and an insufficient number of nucleation sites were available to promote formation of magnetite. However, in biotic batch reactors, the total Fe(II)/Fe(III) ratio for aFh was much lower (0.29) when magnetite was produced, implying the strong influence of bacteria on magnetite transformation.

Role of *S. oneidensis* in Fh transformation. Although bacteria can initiate nucleation of magnetite at low Fe(II) concentration, based on results of final mineral products percentages (Figure 4), the transformations of aFh, bFh-bleach and aFh-HA to magnetite were restricted within the biotic systems compared to the abiotic systems. For instance, the relative amounts of magnetite formed in aFh, bFh-bleach and aFh-HA were lower in biotic systems than abiotic systems (based on Mössbauer spectroscopy data). In biotic systems, magnetite precipitation is catalyzed by the microbial reduction of Fe(III) (i.e. ferrihydrite) which leads to the release of Fe(II) which can further react with Fh to form magnetite. Previous studies have shown that the association of Fe(II) with solid phases can significantly increase the reactivity of the Fe(II), since surface complexation of Fe(II) by hydroxyl groups on the mineral surface stabilizes the Fe(III) oxidation state and can decrease in the Fe(III)-Fe(II) redox potential.³⁷⁻³⁹ In the biotic batch reactors, the reaction between Fe(III) in the solid phase and Fe(II) produced by the bacteria might be inhibited by bacterial cells (*S. oneidensis* MR-1) blocking surface sites, and thus decrease the extent of Fh transformation to magnetite. The passivation of Fh, and/or sequestration of Fe(II) by bacterial cells and associated biomass, such as extracellular polymeric substances (EPS), were confirmed by preliminary experiments of biotic transformation with different cell numbers. *S. oneidensis* MR-1 with a cell number 2×10^9 cells/mL produced more Fe(II)_{total} (4.25 mM; Fe(II)_{total} denotes Fe(II) in aqueous and solid phase) from aFh than that with cell number 1×10^9 cells/mL (3.83 mM) and 5×10^8 cells/mL (3.18 mM) (Figure S4). Additionally, Fe(II)/Fe(III) of Fh transformation with cell number 2×10^9 cells/mL (0.96) was higher than that with cell number 1×10^9 cells/mL (0.7) and 5×10^8 cells/mL (0.52). However, the

MS of Fh transformation with cell number 2×10^9 cells/mL (601×10^{-6}) was much lower than that with cell number 1×10^9 cells/mL (2928×10^{-6}) and 5×10^8 cells/mL (2871×10^{-6}). Mössbauer spectroscopy results were consistent with above Fe concentration which showed 70.5% and 62.3% Fe were present as magnetite transformation products from Fh by *S. oneidensis* MR-1 with cell number 1×10^9 cells/mL and 5×10^8 cells/mL (Figure 3 and Figure S5). However, it is hard to distinguish the sextet present in transformation products from Fh by *S. oneidensis* MR-1 with cell number 2×10^9 cells/mL as being due to either goethite or magnetite due to poor signal to noise ratio. This undefined sextet corresponds to up to 25% Fe present. Therefore, biotic transformation results with different cell numbers suggested bacterial cells and associated biomass, such as EPS, adsorbed/complexed Fe(II), potentially passivated Fh surface and hindered the reaction between Fh and Fe(II). A similar effect has been observed when Fh was inoculated with Fe(III)-reducing bacteria resulting in a decrease of the transformation rate for Fh and spatial heterogeneity of the secondary mineralization products compared to abiotic Fh transformation.⁴⁰⁻⁴³ Additionally, a previous study which explored the effect of a dissolved organic exudate released by Fe(III)-reducing bacteria on the kinetics of Fh transformation (by isolation of the exudate containing Fe(II)) showed that it is the presence of the bacteria cells, and not the exudate alone, which hinders transformation rates of Fh to secondary minerals.⁴⁰

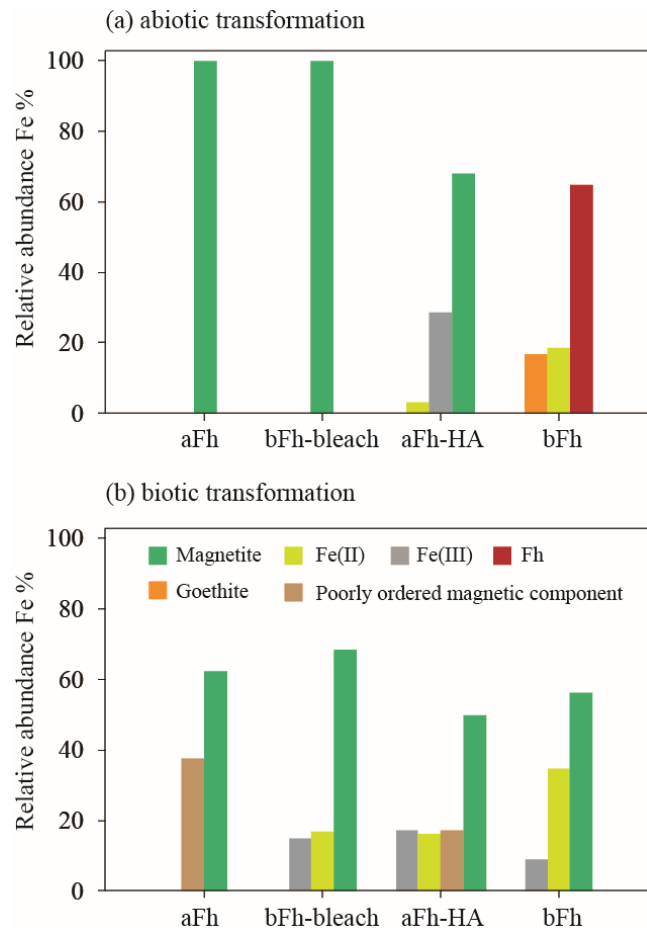


Figure 4. The percentages of transformation products from ferrihydrite induced by $\text{Fe}^{2+}_{\text{aq}}$ abiotically (a) and by *S. oneidensis* MR-1 (b).

Delay between reduction and magnetite formation (Δt). There is a clear lag between the increase of Fe(II)/Fe(III) ratio and the increase of MS for aFh-HA, bFh and bFh-bleach during biotic transformation (Figure 5). This suggests a delay in the order of days to months between the production of Fe(II) by biotic Fe(III) reduction and the precipitation of magnetite. The averaged triplicate values of Fe(II)/Fe(III) ratios in the solids and MS average were fitted with the Hill equation which provided a close approximation to the data (see supplementary information). The first order derivative of the respective model was then calculated to provide information related to the rates of Fe(III) reduction and magnetite formation. The fastest rate of Fe(II)/Fe(III) or MS increase were determined from the maxima of the respective first order derivatives (Figure 5, Table S4). We refer to the difference between maximum rate of

Fe(II)/Fe(III) or MS increase as Δt . There was almost no delay for the three Fh substrates (aFh, aFh-HA, bFh-bleach) which transformed to magnetite during abiotic transformations (Figure S6). In biotic transformations, aFh showed almost no delay (<1 d), while for bFh-bleach, aFh-HA and bFh, the Δt were 19 d, 33 d and ~40 d, respectively. We postulate that the mechanisms which are causing these delays between biotic Fe(III) reduction and magnetite formation include: (i) Fh surface passivation by an organic layer and (ii) complexation of Fe(II) by bacterial cells. An organic layer formed by biomass (from the Fe(II)-oxidizing bacteria which produced the Fh) or HA can block or passivate the surface Fh against reaction with Fe(II), resulting in no direct magnetite production. As mentioned above, bacteria cells adsorbing/complexing with Fe(II) could passivate Fe(II) and hinder the reaction between Fh and Fe(II). We postulate that over time this organic layer and bacteria cells degrade, allowing the reaction between Fe(II) and Fh and initiating transformation to magnetite. Similar results in previous studies showed the strong initial interactions between biogenic organic matter and iron with biogenic organic matter released over the course of days to weeks, eventually allowing the iron minerals to precipitate.⁴⁴⁻⁴⁶

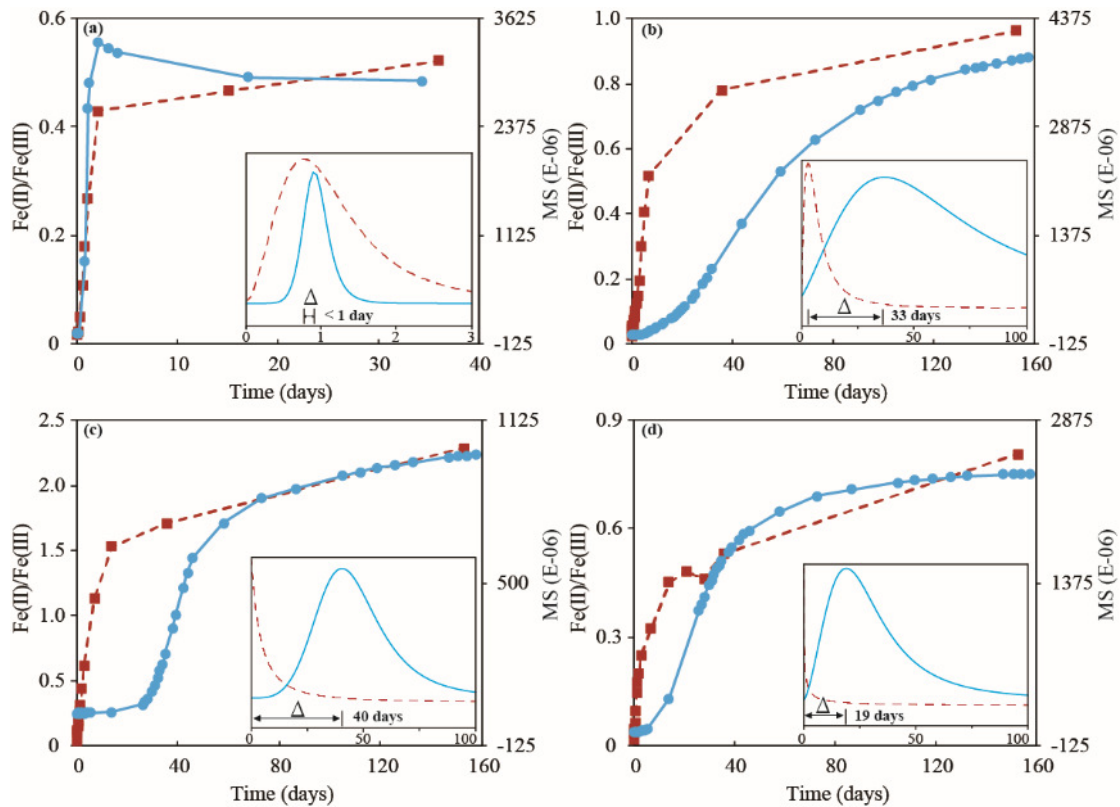


Figure 5. Fe(II)/Fe(III) compared to MS over time in biotic transformation of aFh (a), aFh-HA (b), bFh (c) and bFh-bleach (d). The red and blue lines correspond to Fe(II)/Fe(III) and magnetic susceptibility, respectively. Inserts show the first derivative of Fe(II)/Fe(III) and MS.

Effect of humic acid and biomass on the rates and extent of transformation of Fh. All Fh substrates in both abiotic and biotic experiments transformed to magnetite with the exception of bFh in the abiotic experiment. The bFh underwent further transformation into more thermodynamically stable goethite with no magnetite produced within 64 days in the abiotic experiment. Similar results have been found in other studies which demonstrate organic matter strongly retards or even suppresses Fe(II)-induced abiotic transformation of Fh when exposed OM-Fe coprecipitates with C/Fe molar ratios of ~0.7-4.2 at 0.2–5.0 mM $\text{Fe}^{2+}_{\text{aq}}$.^{18-20, 47-49} Here, the lower C/Fe molar ratio of bFh (0.39) and higher initial $\text{Fe}^{2+}_{\text{aq}}$ concentration (~7 mM) compared with previous studies still appears to limit abiotic Fh transformation, implying the

delaying or even inhibiting effect of biomass on Fh transformation. Although the C/Fe molar ratios of aFh-HA and bFh are similar, the extent of decrease of the Fh transformation rate by microbial biomass is much larger compared with HA. Even when treated with bleach to remove 97% biomass for bFh, the residual biomass or the lower surface reactivity of bFh-bleach due to the bleach treatment still delayed the Fh transformation. The possible mechanisms for the delaying or inhibiting effect of HA and biomass on Fh transformation could be the complexation of Fe(II) by OM which can decrease free $\text{Fe}^{2+}_{\text{aq}}$ concentration in the solution and thus lower secondary mineral transformations of Fh.^{22, 50} However, based on the $\text{Fe}^{2+}_{\text{aq}}$ concentration in our study, there was less $\text{Fe}^{2+}_{\text{aq}}$ removal in abiotic transformation and more $\text{Fe}^{2+}_{\text{aq}}$ in the aqueous phase of biotic transformation for Fh with OM than that without OM, suggesting complexation of Fe(II) by OM is a minor component of our system.

Magnetite forms via solid-state conversion of Fh or via dissolution of Fh and subsequent re-precipitation and/or a combination of both.^{8, 51, 52} For both pathways, adsorption of Fe(II) to Fh is necessary to induce electron transfer and drive the transformation.^{40, 53, 54} Additionally, previous experimental results have also demonstrated that the microbial reduction rate and extent of Fe(III) (oxyhydr)oxides are controlled by the surface area and site concentration of the Fe(III) (oxyhydr)oxides.^{22, 55, 56} HA and biomass partially blocked adsorption sites, and therefore prevented or slowed the transformation of Fh to magnetite. The specific surface area results of the four Fh substrates also confirmed this assumption; the presence of HA and biomass decreased SSA of Fh, and lead to formation of larger aggregates, resulting in the lower accessible surface area per mass ferrihydrite for electron transfer. Recent studies on atom exchange between aqueous $^{57}\text{Fe}(\text{II})$ or $^{56}\text{Fe}(\text{II})$ with Fh-OM show that even though electron transfer still occurs between Fe(II) and Fh-OM, no measurable formation of secondary minerals can be observed.^{20, 57} These results imply that although OM fails to prevent the electron transfer between Fe(II) and Fh-OM, it can retard secondary mineral transformation of Fh by inhibiting Fh aggregation and growth via Ostwald ripening, thus stabilizing Fh. Alternatively, the presence

of HA and biomass can induce a negative surface charge of Fh, which can block sorption of negatively charged cells on Fh surface due to electrostatic repulsion. In summary, both HA and biomass affect Fh mineral properties, such as sorption sites availability, surface area and mineral charge, inducing unique mineral transformation behavior for bFh and aFh-HA from aFh under abiotic and biotic reducing conditions. Additionally, the abiotic transformation products from bFh and aFh-HA were goethite and magnetite respectively, suggesting while the similar mechanisms for the delaying or inhibiting impact of HA and biomass on Fh transformation may be at play, the overall effect of HA vs biomass association with Fh was different.

Environmental implications. The transformation of Fe minerals directly influences Fe cycling as well as the fate of associated nutrients and contaminants. Magnetite formation is of particular interest due to its high reactivity towards pollutants in the environment, and its magnetic properties, which make it as a potential tool for climate reconstruction and organic contaminant detection.^{58, 59} This study advances our understanding of the formation of magnetite under different geochemical settings relevant to the environment. Our work further advances previous studies^{20, 22, 57} which have predominantly focused on the transformation of ferrihydrite and not specifically looked at the rates of magnetite precipitation as we have investigated here. The results of our study highlight the importance of the Fe(II)/Fh ratio in the rate and extent of magnetite formation. Abiotic ferrihydrite transformation to magnetite may not occur in soils and sediments containing extremely low or high Fe(II)/Fh ratios. For example, such a scenario may be expected in the surface water which is fully oxygenated. Additionally, we hypothesized that microbial biomass associated with biogenic Fh could block or inhibit the reaction between Fh and $\text{Fe}^{2+}_{\text{aq}}$ and stabilize Fh; however, Fh remains bioavailable even when associated with biomass, as demonstrated by the transformation to magnetite. However, although the OM-Fh co-precipitates are more stable than pure Fh in natural environment over long periods of time, it can still undergo transformation, especially if there is a shift in the geochemical conditions. Further studies on the bonding between biomass and Fh, such as the sorption vs.

inclusion/occlusion into the structure, as well as the release of OC and variation of magnetite particle sizes during microbial reduction of bFh is needed to make definitive conclusions on the biogeochemical impacts of biomass on Fe cycling.

ASSOCIATED CONTENT

Supporting Information. This information is available free of charge via the Internet at <http://pubs.acs.org>. The supporting materials contain additional Materials and Methods, tables with properties of four initial Fh substrates, Mössbauer spectroscopy hyperfine parameters, Fe(II)/Fe(III) ratio of each of the magnetite formation products determined based on Mössbauer spectroscopy and information for fitted lines of Fe(II)/Fe(III) and MS, figures showing outline of all batch reactors, Mössbauer spectrum of four Fh substrates, MS for abiotic transformation with different Fe(II):Fh ratio, Fe concentration, MS and Mössbauer spectrum for biotic transformation with difference cell numbers, lag phase in abiotic transformation and Hill plots for abiotic and biotic transformation, references (60-62). A separate excel file contains Fe concentration and MS data.

Notes

The authors declare no competing financial interest.

ACKNOWLEDGMENTS

This research was funded by the German Research Foundation (DFG) under grant no. KA 1736/39-1. We also thank China Scholarship Council (CSC) for the financial support to X.H. Yongxin Pan was supported by a grant of the National Natural Science Foundation of China (41621004).

REFERENCES

1. Usman, M.; Byrne, J. M.; Chaudhary, A.; Orsetti, S.; Hanna, K.; Ruby, C.; Kappler, A.; Haderlein, S. B., Magnetite and Green Rust: Synthesis, Properties, and Environmental Applications of Mixed-Valent Iron Minerals. *Chem. Rev.* **2018**, *118*, (7), 3251-3304.
2. Byrne, J. M.; Klueglein, N.; Pearce, C.; Rosso, K. M.; Appel, E.; Kappler, A., Redox cycling of Fe(II) and Fe(III) in magnetite by Fe-metabolizing bacteria. *Science* **2015**, *347*, (6229), 1473.
3. Melton, E. D.; Swanner, E. D.; Behrens, S.; Schmidt, C.; Kappler, A., The interplay of microbially mediated and abiotic reactions in the biogeochemical Fe cycle. *Nature Reviews Microbiology* **2014**, *12*, (12), 797-808.
4. Pankhurst, Q. A.; Connolly, J.; Jones, S. K.; Dobson, J., Applications of magnetic nanoparticles in biomedicine. *J. Phys. D: Appl. Phys.* **2003**, *36*, (13), R167-R181.
5. Su, C., Environmental implications and applications of engineered nanoscale magnetite and its hybrid nanocomposites: A review of recent literature. *J. Hazard. Mater.* **2017**, *322*, 48-84.
6. Byrne, J. M.; Kappler, A., Current and future microbiological strategies to remove As and Cd from drinking water. *Microb. Biotechnol.* **2017**, *10*, (5), 1098-1101.
7. Hansel, C. M.; Benner, S. G.; Neiss, J.; Dohnalkova, A.; Kukkadapu, R. K.; Fendorf, S., Secondary mineralization pathways induced by dissimilatory iron reduction of ferrihydrite under advective flow. *Geochim. Cosmochim. Acta* **2003**, *67*, (16), 2977-2992.
8. Cornell, R. M.; Schwertmann, U., *The iron oxides: structure, properties, reactions, occurrences and uses*. John Wiley & Sons: 2003.
9. Liu, H.; Li, P.; Lu, B.; Wei, Y.; Sun, Y., Transformation of ferrihydrite in the presence or absence of trace Fe(II): The effect of preparation procedures of ferrihydrite. *J. Solid State Chem.* **2009**, *182*, (7), 1767-1771.
10. Ruby, C.; Géhin, A.; Abdelmoula, M.; Génin, J.-M. R.; Jolivet, J.-P., Coprecipitation of Fe(II) and Fe(III) cations in sulphated aqueous medium and formation of hydroxysulphate green rust. *Solid State Sciences* **2003**, *5*, (7), 1055-1062.
11. Byrne, J. M.; Muhamadali, H.; Coker, V.; Cooper, J.; Lloyd, J., Scale-up of the production of highly reactive biogenic magnetite nanoparticles using *Geobacter sulfurreducens*. *Journal of The Royal Society Interface* **2015**, *12*, (107), 20150240.
12. Hansel, C. M.; Benner, S. G.; Fendorf, S., Competing Fe (II)-induced mineralization pathways of ferrihydrite. *Environ. Sci. Technol.* **2005**, *39*, (18), 7147-7153.
13. Fredrickson, J. K.; Zachara, J. M.; Kennedy, D. W.; Dong, H.; Onstott, T. C.; Hinman, N. W.; Li, S.-m., Biogenic iron mineralization accompanying the dissimilatory reduction of hydrous ferric oxide by a groundwater bacterium. *Geochim. Cosmochim. Acta* **1998**, *62*, (19), 3239-3257.
14. Lalonde, K.; Mucci, A.; Ouellet, A.; Gélinas, Y., Preservation of organic matter in sediments promoted by iron. *Nature* **2012**, *483*, 198.
15. Zhao, Q.; Poulson, S. R.; Obrist, D.; Sumaila, S.; Dynes, J. J.; Mcbeth, J. M.; Yang, Y., Iron-Bound Organic Carbon in Forest Soils: Quantification and Characterization. *Biogeosciences Discussions* **2016**, *27*, (2), 1-27.
16. Lovley, D. R., Microbial Fe(III) reduction in subsurface environments. *FEMS Microbiol. Rev.* **1997**, *20*, (3-4), 305-313.
17. Lovley, D. R.; Anderson, R. T., Influence of dissimilatory metal reduction on fate of organic and metal contaminants in the subsurface. *HydJ* **2000**, *8*, (1), 77-88.
18. Jones, A. M.; Collins, R. N.; Rose, J.; Waite, T. D., The effect of silica and natural organic matter on the Fe(II)-catalysed transformation and reactivity of Fe(III) minerals. *Geochim. Cosmochim. Acta* **2009**, *73*, (15), 4409-4422.
19. Chen, C.; Kukkadapu, R.; Sparks, D. L., Influence of Coprecipitated Organic Matter on Fe²⁺(aq)-Catalyzed Transformation of Ferrihydrite: Implications for Carbon Dynamics. *Environ. Sci. Technol.* **2015**, *49*, (18), 10927-10936.
20. ThomasArrigo, L. K.; Byrne, J. M.; Kappler, A.; Kretzschmar, R., Impact of Organic Matter on Iron(II)-Catalyzed Mineral Transformations in Ferrihydrite–Organic Matter Coprecipitates. *Environ. Sci. Technol.* **2018**, *52*, (21), 12316-12326.
21. Han, L.; Sun, K.; Keiluweit, M.; Yang, Y.; Yang, Y.; Jin, J.; Sun, H.; Wu, F.; Xing, B., Mobilization of ferrihydrite-associated organic carbon during Fe reduction: Adsorption versus coprecipitation. *Chemical Geology* **2019**, *503*, 61-68.

22. Shimizu, M.; Zhou, J.; Schröder, C.; Obst, M.; Kappler, A.; Borch, T., Dissimilatory Reduction and Transformation of Ferrihydrite-Humic Acid Coprecipitates. *Environ. Sci. Technol.* **2013**, *47*, (23), 13375-13384.
23. Eusterhues, K.; Hädrich, A.; Neidhardt, J.; Küsel, K.; Keller, T. F.; Jandt, K. D.; Totsche, K. U., Reduction of ferrihydrite with adsorbed and coprecipitated organic matter: microbial reduction by *Geobacter bremensis* vs. abiotic reduction by Na-dithionite. *Biogeosciences* **2014**, *11*, (18), 4953-4966.
24. Amstatter, K.; Borch, T.; Kappler, A., Influence of humic acid imposed changes of ferrihydrite aggregation on microbial Fe(III) reduction. *Geochim. Cosmochim. Acta* **2012**, *85*, 326-341.
25. Emerson, D.; Weiss, J. V., Bacterial Iron Oxidation in Circumneutral Freshwater Habitats: Findings from the Field and the Laboratory. *Geomicrobiology Journal* **2004**, *21*, (6), 405-414.
26. Emerson, D.; Fleming, E. J.; McBeth, J. M., Iron-Oxidizing Bacteria: An Environmental and Genomic Perspective. *Annu. Rev. Microbiol.* **2010**, *64*, (1), 561-583.
27. Duckworth, O. W.; Holmström, S. J. M.; Peña, J.; Sposito, G., Biogeochemistry of iron oxidation in a circumneutral freshwater habitat. *Chemical Geology* **2009**, *260*, (3), 149-158.
28. Sowers, T. D.; Holden, K. L.; Coward, E. K.; Sparks, D. L., Dissolved Organic Matter Sorption and Molecular Fractionation by Naturally Occurring Bacteriogenic Iron (Oxyhydr)oxides. *Environ. Sci. Technol.* **2019**, *53*, (8), 4295-4304
29. Raven, K. P.; Jain, A.; Loeppert, R. H., Arsenite and Arsenate Adsorption on Ferrihydrite: Kinetics, Equilibrium, and Adsorption Envelopes. *Environ. Sci. Technol.* **1998**, *32*, (3), 344-349.
30. Hegler, F.; Posth, N. R.; Jiang, J.; Kappler, A., Physiology of phototrophic iron (II)-oxidizing bacteria: implications for modern and ancient environments. *FEMS Microbiol. Ecol.* **2008**, *66*, (2), 250-260.
31. Lavkulich, L. M.; Wiens, J. H., Comparison of organic matter destruction by hydrogen peroxide and sodium hypochlorite and its effects on selected mineral constituents. *Soil Science Society of America Journal* **1970**, *34*, (5), 755-758.
32. Stookey, L. L., Ferrozine---a new spectrophotometric reagent for iron. *Analytical Chemistry* **1970**, *42*, (7), 779-781.
33. Rancourt, D. G.; Ping, J. Y., Voigt-based methods for arbitrary-shape static hyperfine parameter distributions in Mössbauer spectroscopy. *Nuclear Instruments and Methods in Physics Research Section B: Beam Interactions with Materials and Atoms* **1991**, *58*, (1), 85-97.
34. Porsch, K.; Dippon, U.; Rijal, M. L.; Appel, E.; Kappler, A., In-Situ Magnetic Susceptibility Measurements As a Tool to Follow Geomicrobiological Transformation of Fe Minerals. *Environ. Sci. Technol.* **2010**, *44*, (10), 3846-3852.
35. Dunlop, D. J.; Özdemir, Ö., *Rock magnetism: fundamentals and frontiers*. Cambridge university press: 2001; Vol. 3.
36. Gorski, C. A.; Scherer, M. M., Determination of nanoparticulate magnetite stoichiometry by Mössbauer spectroscopy, acidic dissolution, and powder X-ray diffraction: A critical review. *American Mineralogist* **2010**, *95*, (7), 1017-1026.
37. Pecher, K.; Haderlein, S. B.; Schwarzenbach, R. P., Reduction of Polyhalogenated Methanes by Surface-Bound Fe(II) in Aqueous Suspensions of Iron Oxides. *Environ. Sci. Technol.* **2002**, *36*, (8), 1734-1741.
38. Elsner, M.; Schwarzenbach, R. P.; Haderlein, S. B., Reactivity of Fe(II)-Bearing Minerals toward Reductive Transformation of Organic Contaminants. *Environ. Sci. Technol.* **2004**, *38*, (3), 799-807.
39. Stumm, W.; Sulzberger, B.; Sinniger, J., The coordination chemistry of the oxide-electrolyte interface; the dependence of surface reactivity (dissolution, redox reactions) on surface structure. *Croat. Chem. Acta* **1990**, *63*, (3), 277-312.
40. Xiao, W.; Jones, A. M.; Li, X.; Collins, R. N.; Waite, T. D., Effect of *Shewanella oneidensis* on the Kinetics of Fe(II)-Catalyzed Transformation of Ferrihydrite to Crystalline Iron Oxides. *Environ. Sci. Technol.* **2018**, *52*, (1), 114-123.
41. Pallud, C.; Kausch, M.; Fendorf, S.; Meile, C., Spatial Patterns and Modeling of Reductive Ferrihydrite Transformation Observed in Artificial Soil Aggregates. *Environ. Sci. Technol.* **2010**, *44*, (1), 74-79.
42. Pallud, C.; Masue-Slowey, Y.; Fendorf, S., Aggregate-scale spatial heterogeneity in reductive transformation of ferrihydrite resulting from coupled biogeochemical and physical processes.

- Geochim. Cosmochim. Acta* **2010**, *74*, (10), 2811-2825.
43. Dippon, U.; Schmidt, C.; Behrens, S.; Kappler, A., Secondary Mineral Formation During Ferrihydrite Reduction by *Shewanella oneidensis* MR-1 Depends on Incubation Vessel Orientation and Resulting Gradients of Cells, Fe²⁺ and Fe Minerals. *Geomicrobiology Journal* **2015**, *32*, (10), 878-889.
 44. Adhikari, D.; Zhao, Q.; Das, K.; Mejia, J.; Huang, R.; Wang, X.; Poulson, S. R.; Tang, Y.; Roden, E. E.; Yang, Y., Dynamics of ferrihydrite-bound organic carbon during microbial Fe reduction. *Geochim. Cosmochim. Acta* **2017**, *212*, (Supplement C), 221-233.
 45. Pan, W.; Kan, J.; Inamdar, S.; Chen, C.; Sparks, D., Dissimilatory microbial iron reduction release DOC (dissolved organic carbon) from carbon-ferrihydrite association. *Soil Biol. Biochem.* **2016**, *103*, 232-240.
 46. Chan, C. S.; Fakra, S. C.; Edwards, D. C.; Emerson, D.; Banfield, J. F., Iron oxyhydroxide mineralization on microbial extracellular polysaccharides. *Geochim. Cosmochim. Acta* **2009**, *73*, (13), 3807-3818.
 47. Pasakarnis, T. S., Effects of carbon during Fe (II)-catalyzed Fe oxide recrystallization: implications for Fe and carbon cycling. **2013**.
 48. Henneberry, Y. K.; Kraus, T. E. C.; Nico, P. S.; Horwath, W. R., Structural stability of coprecipitated natural organic matter and ferric iron under reducing conditions. *Organic Geochemistry* **2012**, *48*, 81-89.
 49. Xiao, W.; Jones, A. M.; Collins, R. N.; Waite, T. D., Investigating the effect of ascorbate on the Fe(II)-catalyzed transformation of the poorly crystalline iron mineral ferrihydrite. *Biochimica et Biophysica Acta (BBA) - General Subjects* **2018**, *1862*, (8), 1760-1769.
 50. ThomasArrigo, L. K.; Mikutta, C.; Byrne, J.; Kappler, A.; Kretzschmar, R., Iron(II)-Catalyzed Iron Atom Exchange and Mineralogical Changes in Iron-rich Organic Freshwater Floes: An Iron Isotope Tracer Study. *Environ. Sci. Technol.* **2017**, *51*, (12), 6897-6907.
 51. Tronc, E.; Belleville, P.; Jolivet, J. P.; Livage, J., Transformation of ferric hydroxide into spinel by iron(II) adsorption. *Langmuir* **1992**, *8*, (1), 313-319.
 52. Bazylinski, D. A.; Frankel, R. B.; Konhauser, K. O., Modes of Biomineralization of Magnetite by Microbes. *Geomicrobiology Journal* **2007**, *24*, (6), 465-475.
 53. Jolivet, J. P.; Belleville, P.; Tronc, E.; Livage, J., Influence of Fe(II) on the Formation of the Spinel Iron Oxide in Alkaline Medium. *Clays Clay Miner.* **1992**, *40*, (5), 531-539.
 54. Elisabeth, T.; Philippe, B.; Jolivet, J.-P., Transformation of Ferric Hydroxide Into Spinel by Fe(II) Adsorption [J]. *Langmuir* **1992**, *8*, 313.
 55. Roden, E. E.; Zachara, J. M., Microbial Reduction of Crystalline Iron(III) Oxides: Influence of Oxide Surface Area and Potential for Cell Growth. *Environ. Sci. Technol.* **1996**, *30*, (5), 1618-1628.
 56. Roden, E. E., Fe(III) Oxide Reactivity Toward Biological versus Chemical Reduction. *Environ. Sci. Technol.* **2003**, *37*, (7), 1319-1324.
 57. Zhou, Z.; Latta, D. E.; Noor, N.; Thompson, A.; Borch, T.; Scherer, M. M., Fe(II)-Catalyzed Transformation of Organic Matter–Ferrihydrite Coprecipitates: A Closer Look Using Fe Isotopes. *Environ. Sci. Technol.* **2018**, *52*, (19), 11142-11150.
 58. Porsch, K.; Rijal, M. L.; Borch, T.; Troyer, L. D.; Behrens, S.; Wehland, F.; Appel, E.; Kappler, A., Impact of organic carbon and iron bioavailability on the magnetic susceptibility of soils. *Geochim. Cosmochim. Acta* **2014**, *128*, 44-57.
 59. Ahmed, I. A. M.; Maher, B. A., Identification and paleoclimatic significance of magnetite nanoparticles in soils. *Proceedings of the National Academy of Sciences* **2018**, *115* (8), 1736-1741.